

SNR improvement of 8.2 dB in a self-mixing laser diode interferometer by using the difference signal at the output mirrors [Invited]

Silvano Donati^{1*} and Michele Norgia²

¹Department of Industrial and Information Engineering, University of Pavia, 27100 Pavia, Italy

²Department of Electronics, Informatics and Bioengineering, 20133 Milano, Italy

*Corresponding author: silvano.donati@unipv.it

Received April 14, 2021 | Accepted May 14, 2021 | Posted Online July 8, 2021

At the mirrors of a laser diode self-mixing interferometer, the output beams carry anti-correlated (i.e., in phase opposition) interferometric signals, whereas the superposed noise fluctuations are (partially) correlated. Therefore, by using an instrumental output of the interferometer as the difference of the two, we double the amplitude of the self-mixing useful signal, while the superposed noise is reduced. To validate the idea, we first calculate the noise reduction by means of a second-quantization model, finding that in a laser diode the signal-to-noise ratio (SNR) can be improved by 8.2 dB, typically. Then, we also carry out an experimental measurement of SNR and find very good agreement with the theoretical result.

Keywords: interferometry; self-mixing; noise; laser diodes.

DOI: [10.3788/COL202119.092502](https://doi.org/10.3788/COL202119.092502)

1. Introduction

The self-mixing interferometer (SMI) is a well-known minimum-part configuration of interferometry based on the modulations of the cavity field induced by weak return from the target under measurement^[1]. The modulation indices are the signals $\cos(2k\Delta s)$ and $\sin(2k\Delta s)$ (with $k = 2\pi/\lambda$ and s being distance to the target) for the amplitude modulation (AM) and frequency modulation (FM), respectively, which are necessary to trace back, unambiguously, the displacement Δs ^[2]. As the process is coherent, the SMI can work well even with very minute returns (e.g., down to 10^{-8} of emitted power). This feature, coupled to the simplicity of the setup (no external optical parts required, in principle), has led to the development of a number of applications of SMI in the fields of mechanical metrology, biomedical signal sensing, physical quantity measurements, and consumer products, see, e.g., Refs. [1,3] for reviews.

With detection and processing of the modulated signal, usually the AM component is preferred because it is readily available on the laser beam power and conveniently detected by the monitor photodiode (PD) usually provided by the manufacturer on the rear mirror of the laser package. Using AM, we can make digital or analogue processing of the SMI signal, respectively, count fringes of half-wavelengths for displacement measurement and/or to sense vibrations with an output analogue replica of the signal $s(t)$ waveform, down to a fraction of the wavelength and even much less with appropriate circuits^[2,3].

One specific feature of the SMI is that the interferometric signal is carried by the beam. It is found not only on the rear output where the monitor PD2 is placed (see Fig. 1), but also on the front output, where it can be picked up by a beamsplitter (BS) and PD1, as well as on the target itself (not shown in Fig. 1) and on the returning beam by means of PD1'.

Placing the detecting PD on the target allows us to exploit a unique property of the SMI, namely, measuring the displacement or vibration of a target from the target location itself while it is moving, but this possibility will not be developed in this paper. Another special feature of SMI with a semiconductor laser is the availability of the signal across the anode-cathode terminals of the laser diode (not shown in Fig. 1), which in this case works also as a detector—a feature demonstrated for SMI operation at terahertz (THz) frequency^[4]. More commonly, however the rear PD2 signal is used because it is normally already available in the laser diode package, and it does not obstruct the path of propagation to the remote target.

Also, the placement of the detector on the front beam output is interesting, because the signal here is in phase opposition to that detected at the rear mirror in semiconductor laser diodes driven well above threshold, as found by the analysis presented in Ref. [5].

Therefore, with the difference signal of the two outputs, the amplitude of the SMI signal improves by a factor of two, as experimentally verified in Ref. [6].

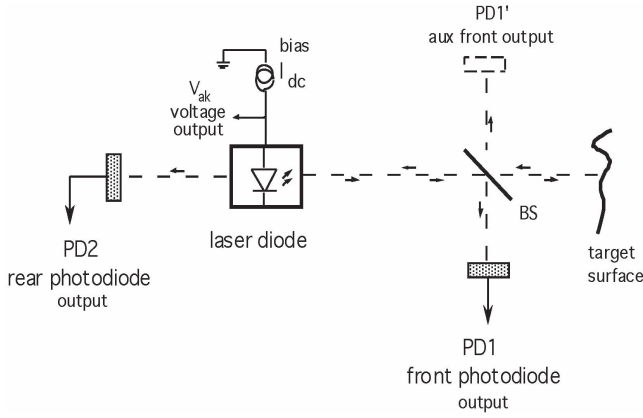


Fig. 1. Different pickups of the output signal from an SMI: from rear PD2 and from front mirrors PD1 and PD1'.

Additionally, it is reasonable to expect that the two outputs, which are generated by the same optical field E_0 traveling back and forth in the laser cavity, are affected by the same noise carried by E_0 (that is to say, the two output noises are correlated). Thus, the difference signal has less noise than the two SMI signals, or its signal-to-noise ratio (SNR) is further improved.

If this conjecture proves correct, the performance of the SMI is improved in its ultimate sensitivity or detectable noise-equivalent-displacement (NED)^[2].

In this paper, we analyze the noise of the two outputs (front and rear) and their difference with a semiclassical noise model^[7], which accounts for second quantization and find that indeed the two outputs have a partial correlation of noise and that the SNR can be improved up to about 10 dB by the differential signal. Then, we test the theoretical results with a 650 nm laser diode SMI and are able to measure an 8.2 dB improvement of SNR, which is in good agreement with theory.

2. Theoretical Model and Analysis

To avoid unnecessary complications, we consider the simplified scheme of Fig. 2 to evaluate the signal and noise of the front and rear outputs of the laser diode, with the photodetectors placed directly on the outputs of the laser. The power reflectivities of mirrors M1 and M2 are R_1 and R_2 , the powers exiting from mirrors are P_1 and P_2 , and they are converted into electrical current signals $I_1 = \sigma P_1$ and $I_2 = \sigma P_2$ by PD1 and PD2. We suppose that PD2 is totally absorbing and PD1 is partially reflecting, so as to act as the target and generate the feedback field re-entering the

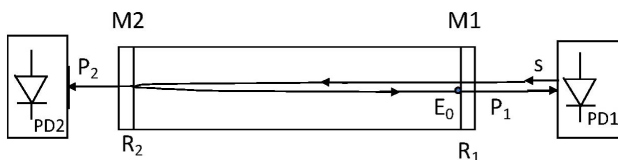


Fig. 2. Simplified scheme of an SMI for the evaluation of front and rear output signals and noise.

laser cavity after propagation to distance s and the accumulated optical phase shift $\phi = 2ks$.

The output power P is related to the electrical field amplitude E by the well-known Poynting's relation $P = aE^2/2Z_0$, where a is the cross-section area of the beam, and Z_0 is the vacuum impedance. In the following, however, we write simply $P_1 = E_1^2$ and $P_2 = E_2^2$ for the powers exiting at mirrors M1 and M2.

Now, we want to calculate the quiescent amplitude of the fields E_1 and E_2 as a function of the unperturbed internal field E_0 and their SMI amplitude variations ΔE_1 and ΔE_2 due to a feedback from the target at distance s returning into the cavity with a fraction A of the field E_0 (taken just before M1, see Fig. 2). The problem was solved in Ref. [5] with the following result for the output field amplitudes E_1 and E_2 when perturbed by a small return AE_0 from the target along a phase shift $\phi = 2ks$:

$$E_1 = t_1 E_0 \{1 - (t_1^2/r_1)(A \cos \phi) [(2\gamma L + \ln R_1 R_2)^{-1} - R_1/T_1]\}, \quad (1)$$

$$E_2 = \sqrt{(r_1/r_2)t_2} E_0 [1 - (t_1^2/r_1)(A \cos \phi) (2\gamma L + \ln R_1 R_2)^{-1}], \quad (2)$$

where A is the attenuation suffered by the field signal on the go-and-return path; $\phi = 2ks$ is the optical phase accumulated in the path to the target and back, with $k = 2\pi/\lambda$ the wavevector and s the target distance; $r_{1,2} = \sqrt{R_{1,2}}$ and $t_{1,2} = \sqrt{R} = T_{1,2}$ are the field reflection and transmission of mirrors M1 and M2, respectively; $2\gamma L$ is the round-trip gain along the laser cavity of length L ; and factor one in curl parentheses indicates the quiescent (or unperturbed) value of the field, to which the AM term induced by the self-mixing is added.

From Eqs. (1) and (2), we can calculate the modulation indices m_1 and m_2 , defined as the ratio of the SMI signal (the term added to unity) and the constant unperturbed field superposed to them, $E_{1,2}$ for $A = 0$, and the result is

$$m_1 = (t_1^2/r_1)(A \cos \phi) [(2\gamma L + \ln R_1 R_2)^{-1} - R_1/T_1], \quad (3)$$

$$m_2 = (t_1^2/r_1)(A \cos \phi) (2\gamma L + \ln R_1 R_2)^{-1}; \quad (4)$$

hence, the ratio

$$m_1/m_2 = 1 - (R_1/T_1)(2\gamma L + \ln R_1 R_2). \quad (5)$$

Because of Eq. (5), the outputs are in phase ($m_1/m_2 = 1$) at threshold ($2\gamma L = -\ln R_1 R_2$), then, in normal operating conditions above threshold, $2\gamma L + \ln R_1 R_2 > T_1/R_1$, and the outputs become in phase opposition (m_1/m_2 negative, typically ≈ -3). The difference in modulation indices of the rear and front outputs is explained by the extra contribution, in the front output, coming from the reflection; on the front mirror, the field returns from the remote target.

In practical operation of a laser diode, the amplitudes of the constant component upon which the SMI is superposed can be brought to the same value, let us say one, by (noiseless)

amplification. Then, the SMI signal amplitudes are given just by the modulation indices of Eqs. (3) and (4).

An interesting feature of these dependences is that the difference signal is twice the semi-sum of (absolute) amplitudes as soon as one of the two changes its sign, the case of m_1 at increasing bias. To see this, let us write Eqs. (3) and (4) in the form: $m'_1 = g - r$, and $m'_2 = g$. Then, the difference signal is $m'_1 - m'_2 = -r$ at all times. But, when m'_1 changes its sign, its (positive) amplitude is $r - g$ and the semi-sum is $\frac{1}{2}(m'_1 + m'_2) = r/2$; accordingly, the ratio $|(m'_1 - m'_2)|/\frac{1}{2}(m'_1 + m'_2)$ is equal to two (in absolute value). For clarity, a numerical example about this statement is provided in Appendix A.

In conclusion, although the amplitudes of the SMI output signals and their ratio [Eq. (5)] may change with gain γ —or with bias current—their difference is always double the average (or semi-sum) amplitude of the output signals.

3. Noise Model and Calculations

We model the SMI noise with the scheme of Fig. 3 bottom, which is rigorous from the point of view of second quantization, as described in Ref. [7]. The oscillating field E_0 is assumed constant in the cavity, and the coherent state fluctuation ΔE_{coh} is attributed to it. The fluctuation ΔE_{coh} is a Gaussian noise of amplitude such that the power $P_0 = aE_0^2/2Z_0$ carried by the field E_0 has the classical quantum (or shot) noise, $\sigma_p^2 = 2h\nu P_0 B$, where B is the bandwidth of observation^[6]. Explicitly, the fluctuation ΔE_{coh} has zero average, $\langle \Delta E_{\text{coh}} \rangle = 0$, and a quadratic mean value given by $\langle \Delta E_{\text{coh}}^2 \rangle = (a/2Z_0)\frac{1}{2}h\nu B$, or, also, a power spectral density $d\langle \Delta E_{\text{coh}}^2 \rangle/df = \frac{1}{2}h\nu$ of a half-photon per hertz. In the following, we omit for simplicity the factor $a/2Z_0$.

Additional to the noise carried by the oscillating field, we shall consider also noises entering the unused port of BSs and partially reflecting mirrors. Indeed, for the second quantization, every port left unused is actually a port left open to the vacuum state fluctuation; that is, a field fluctuation, let us call it ΔE_{vac} (see

Fig. 3), is equal to the coherent state fluctuation, $\Delta E_{\text{vac}} = \Delta E_{\text{coh}}$, consistent with the fact that the coherent state fluctuation ΔE_{coh} is independent from the value of the field E_0 and is therefore found also where it is $E_0 = 0$, i.e., at unused ports^[7].

With the addition of $\Delta E_{\text{vac}1}$ and $\Delta E_{\text{vac}2}$ in Fig. 3, the noise model is complete^[7], and we can calculate the fluctuations of output fields E_1 and E_2 as well as the variance of noises superposed to output powers P_1 and P_2 .

In the classical picture, the output powers P_1 and P_2 are affected by the shot noise due to the Poisson distribution of photons that are carried along, and the variance of the power fluctuation is given by the well-known shot-noise expression $\sigma_p^2 = 2h\nu PB$. As it is generated by the same power P_0 traveling back and forth in the cavity, the powers P_1 and P_2 have some correlation in their shot-noise fluctuation, but not complete correlation because the mirrors select at random which photon is transmitted and which is reflected.

In the following, we calculate the variances $\sigma_{P_1}^2$ and $\sigma_{P_2}^2$ for the two outputs, as made up by two terms each: one totally correlated and another totally uncorrelated to the corresponding term of the other output, so that the first can be cancelled out in a differential operation, and we can evaluate the SNR improvement thereafter.

With reference to Fig. 3, let us now compute mean value and variance of power delivered at output 1, $P_1 = \langle E_1^2 \rangle$ (having omitted for simplicity the multiplying term $a/2Z_0$); also, for simplicity, let us assume equal mirror reflectivity, $R_1 = R_2 = R$. Then, at mirror M_1 , we can write

$$E_1 = t(E_0 + \Delta E_{\text{coh}}) + ir\Delta E_{\text{vac}1}, \quad (6)$$

where $t = \sqrt{T}$ and $r = \sqrt{R}$ are the field transmission and reflection coefficients of the mirrors, ΔE_{coh} is the Gaussian, zero average, and field fluctuation affecting E_0 (and independent from amplitude E_0), and $\Delta E_{\text{vac}1}$ is the same distribution, but uncorrelated to ΔE_{coh} , which enters as the vacuum fluctuation^[7] from the unused port of the BS. The properties are

$$\langle \Delta E_{\text{coh}} \rangle = \langle \Delta E_{\text{vac}1} \rangle = 0, \quad \text{and} \quad \sigma_E^2 = \langle \Delta E_{\text{coh}}^2 \rangle = \langle \Delta E_{\text{vac}1}^2 \rangle = \frac{1}{2}h\nu B. \quad (7)$$

Now, the mean value of P_1 is given by the classical expression $P_1 \propto E^2$ but subtracted from the square average of the vacuum field (because this cannot be observed)^[7]:

$$P_1 = \langle |E_1|^2 \rangle - \langle \Delta E_{\text{vac}1}^2 \rangle. \quad (8)$$

Inserting Eq. (6) into Eq. (8) we get

$$P_1 = t^2 E_0^2 + t^2 \langle \Delta E_{\text{coh}}^2 \rangle + r^2 \langle \Delta E_{\text{vac}1}^2 \rangle + 2t^2 \langle E_0 \Delta E_{\text{coh}} \rangle + 2tr \langle E_0 \Delta E_{\text{vac}1} \rangle + 2tr \langle \Delta E_{\text{coh}} \Delta E_{\text{vac}1} \rangle - \langle \Delta E_{\text{vac}1}^2 \rangle, \quad (9)$$

and, because the second, third, seventh, and the last terms on the right-hand side cancel out, we get

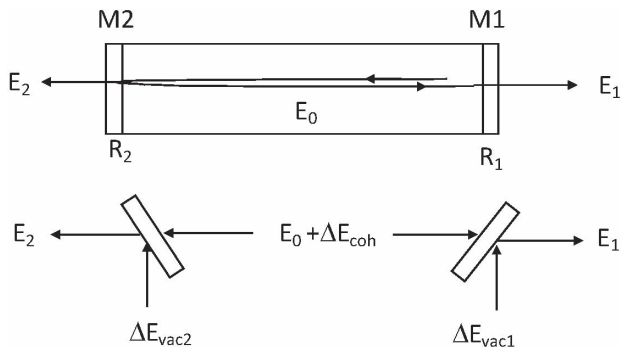


Fig. 3. Top: the laser diode cavity has mirrors with (power) reflectivity R_1 and R_2 , and the optical oscillating field E_0 is assumed constant inside the cavity; bottom: the second-quantization model, in which field E_0 is accompanied by the coherent state fluctuation ΔE_{coh} , and the vacuum state fluctuations $\Delta E_{\text{vac}1,2}$ enter in the unused port of the mirrors, described as a BS because they have non-unitary transmission.

$$\langle P_1 \rangle = t^2 E_0^2 + 2t^2 \langle E_0 E_{\text{coh}} \rangle + 2tr \langle E_0 E_{\text{vac1}} \rangle + 2tr \langle E_{\text{coh}} E_{\text{vac1}} \rangle.$$

As the mean value of E_{coh} and E_{vac1} is zero, E_{coh} and E_{vac1} are uncorrelated, and, noting that $E_0^2 = P_0$ and $t^2 = T$, we get

$$\langle P_1 \rangle = t^2 E_0^2 = TP_0, \quad (10)$$

i.e., just the expected result.

Variance is calculated as the difference $\sigma_{P_1}^2 = \langle P_1^2 \rangle - \langle P_1 \rangle^2$, or $\sigma_{P_1}^2 = t^4 E_0^4 + 4t^2 \langle E_0^2 E_{\text{coh}}^2 \rangle + 4t^2 r^2 \langle E_0^2 E_{\text{vac1}}^2 \rangle - t^4 E_0^4 +$ vanishing double products.

Substituting $t^2 = T$ and $r^2 = R$, we get

$$\sigma_{P_1}^2 = 4T^2 E_0^2 \langle E_{\text{coh}}^2 \rangle + 4TR E_0^2 \langle E_{\text{vac1}}^2 \rangle, \quad (11)$$

and, using $TE_0^2 = P_1$ and $\langle E_{\text{coh}}^2 \rangle = \langle E_{\text{vac1}}^2 \rangle = \frac{1}{2} h\nu B$, we finally obtain

$$\sigma_{P_1}^2 = 2TP_1 h\nu B + 2RP_1 h\nu B. \quad (12)$$

Worth noting, as $R + T = 1$, Eq. (12) is also written as $\sigma_{P_1}^2 = 2P_1 h\nu B$, that is, the classical variance expected for a Poisson-statistics power P_1 .

Now, we can repeat the calculation for exit 2, and it is straightforward to write the result as

$$\begin{aligned} P_2 &= P_1, \\ \sigma_{P_2}^2 &= 4T^2 E_0^2 \langle E_{\text{coh}}^2 \rangle + 4TRE_0^2 \langle E_{\text{vac2}}^2 \rangle \\ &= 2TP_2 h\nu B + 2RP_2 h\nu B. \end{aligned} \quad (13)$$

Note that the first right-hand side terms of Eqs. (12) and (13) are the same as those derived from the same process, the beating of signal with its coherent state fluctuation, so they are completely correlated and will be canceled out, making the difference $P = P_1 - P_2$. Instead, the second right-hand side terms of Eqs. (12) and (13) are completely uncorrelated because they come from different independent fluctuations, E_{vac1} and E_{vac2} .

Taking account of the correlations, we get the variance of $P = P_1 - P_2$,

$$\begin{aligned} \sigma_{P_2-P_1}^2 &= 4TRE_0^2 \langle E_{\text{vac1}}^2 \rangle + 4TRE_0^2 \langle E_{\text{vac2}}^2 \rangle \\ &= 8TRP_0 \frac{1}{2} h\nu B = 4RP_1 h\nu B \end{aligned} \quad (14)$$

to be compared to $\sigma_{P_1}^2 = \sigma_{P_2}^2 = 2P_1 h\nu B$. Therefore, the ratio of free and differential variance is

$$\sigma_{P_2-P_1}^2 / \sigma_{P_1}^2 = 2R, \quad (15)$$

and the corresponding SNR, considering the doubling of the differential signal becomes

$$F = (\text{SNR}_{P_2-P_1} / \text{SNR}_{P_1})^2 = (4/2R)/1 = 2/R. \quad (16)$$

For a semiconductor laser with a typical $R = 0.3$, we get

$$F = 2/0.3 = 6.6 \text{ (or 8.2 dB)}.$$

About the output voltage signal $V = R_{tr} \sigma P$ obtained across a resistance R fed by the PD current $I = \sigma P$, we have for the SNR the same ratio, or

$$\begin{aligned} (\text{SNR}_{P_2-P_1} / \text{SNR}_{P_1})^2 &= (\text{SNR}_{V_2-V_1} / \text{SNR}_{V_1})^2 \text{ or also} \\ \text{SNR}_{V_2-V_1} / \text{SNR}_{V_1} &= \sqrt{F}, \quad \text{and} \\ 20 \log \sqrt{F} &= 10 \log F = 8.2 \text{ dB}. \end{aligned}$$

For a He–Ne laser, the front and rear outputs are in phase, in the normal operation of the source^[5], so the factor two of the differential outputs is not achieved, and we have $F = 1/R$. Moreover, as the reflection coefficient of typical He–Ne mirrors is $R = 0.95\text{--}0.98$, the improvement in F is marginal.

With a slightly different method based on second quantization, Elsasser and coworkers^[8] have calculated the correlations of the output fields in a Fabry–Perot laser, including the effects of internal absorption and spatial hole burning, with the aim of generating correlated light beams, and found correlation factors up to 0.8. The low-frequency suppression of $1/f$ components in a laser diode by output subtraction has been investigated by Fronen^[9] finding almost complete correlation between the two outputs.

3.1. Extension of the noise results

Usually, Fabry–Perot semiconductor lasers have cleaved facets, so $R_1 = R_2$ and the results of previous sections apply. However, one can come across lasers with $R_1 \neq R_2$, and, therefore, we extend the theory to the general case of different mirror reflectivity.

By repeating the calculations of previous sections, we find that, upon equalizing the output power amplitudes, the variance of the output difference is given by

$$\sigma_{P_2-P_1}^2 = 2(R_2 T_1 + R_1 T_2) \sqrt{(R_1 R_2) P_{00} h\nu B},$$

where P_{00} is the power at the crossover point internal to the laser, at which left-going and right-going beams are of equal power. Moreover, the variances of the outputs—after balancing the mean power signal—are

$$\sigma_{P_1 \text{ or } 2}^2 = 2\sqrt{(T_1 T_2)} \sqrt{(R_1 R_2) P_{00} h\nu B};$$

hence, the variance ratio becomes

$$\sigma_{P_2-P_1}^2 / \sigma_{P_1 \text{ or } 2}^2 = (R_2 T_1 + R_1 T_2) / \sqrt{T_1 T_2}, \quad (17)$$

for $R_2 = R_1 = R$, and $T_1 = T_2 = T$, and Eq. (17) gives the same as Eq. (15). Also, the improvement in SNR is given by $F = 2\sqrt{(T_1 T_2)} / (R_2 T_1 + R_1 T_2)$, which becomes $F = 1/2R$ for equal R and T .

3.2. Picking the front output signal

As mentioned above, the receiving PD placed on the front output of mirror M1 can also serve, with its transparent window

reflecting a few percent of the incoming radiation, as the target surface while intercepting practically all of the power P_1 available. However, when this arrangement is not allowed by the application, normally because of its invasiveness, we can use either a BS, deviating a fraction of the power in transit to the P1, as shown in Fig. 4 (top), or a partial removal of the outgoing beam (see below).

The BS offers a compact solution to power pickup, because it may be as small as the beam, but has the serious disadvantage of opening a port to the vacuum fluctuation, term ΔE_{vacBS} in Fig. 4 (bottom).

The calculation of powers and associated variances follows the guidelines of previous sections, and, for brevity, we will omit here the detailed development of the analysis, limiting ourselves to report the results. For $R_1 = R_2 = R$, it is found that the power at the detector PD1 is given by

$$P_{1BS} = (r_{BS}t)^2 E_0^2 = R_{BS}P_1 = TR_{BS}P_0, \quad (18)$$

while the power at the other mirror is still $P_1 = t^2 E_0^2 = TP_0$, larger than P_{1BS} , and this circumstance will generally require a balance operation to get equal amplitude levels. The variance of fluctuations associated with P_{1BS} is

$$\begin{aligned} \sigma_{P_{1BS}}^2 &= 2TR_{BS}P_{1BS}h\nu B + 2(RR_{BS} + T_{BS})P_{1BS}h\nu B \\ &= 2TR_{BS}^2P_1h\nu B + 2R_{BS}(RR_{BS} + T_{BS})P_1h\nu B. \end{aligned} \quad (19)$$

After the (noiseless) power amplification by factor $1/R_{BS}$ to equalize the amplitude of P_{1BS} before subtracting P_2 , so that we obtain $P_1 - P_2 = 2P_1$, we get the equalized variance $\sigma_{P_{1BS}(eq)}$:

$$\begin{aligned} \sigma_{P_{1BS}(eq)}^2 &= \sigma_{P_{1BS}}^2/R_{BS}^2 \\ &= [2TR_{BS}^2P_1h\nu B + 2R_{BS}(RR_{BS} + T_{BS})P_1h\nu B]/R_{BS}^2 \\ &= 2TP_1h\nu B + 2(R + T_{BS}/R_{BS})P_1h\nu B \end{aligned} \quad (20)$$

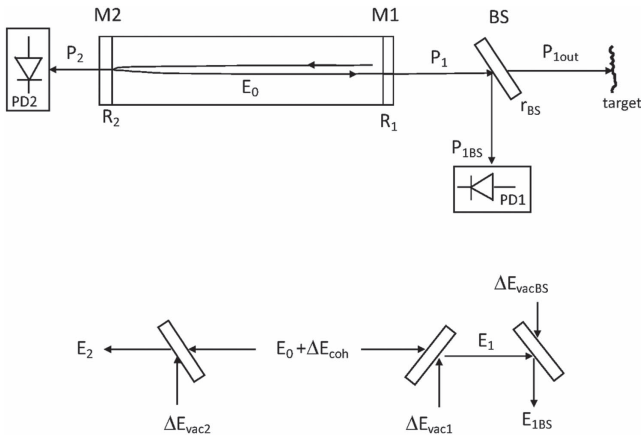


Fig. 4. (top) Pickup of the front SMI signal by means of a BS, deviating a fraction R_{BS} of power P_1 to PD1; (bottom) equivalent circuit for the evaluation of noise, showing the added fluctuation ΔE_{vacBS} entering in the unused port of the BS.

to be compared with

$$\sigma_{P_1}^2 = 2TP_1h\nu B + 2RP_1h\nu B,$$

where the first terms (correlated) cancel out again, and the second terms give the difference as

$$\begin{aligned} \sigma_{P_2-P_1}^2 &= 2(2R + T_{BS}/R_{BS})P_1h\nu B, \\ \text{and } \text{SNR}_{P_1-P_2}^2 &= [4/2(2R + T_{BS}/R_{BS})](P_1h\nu B) \\ &= [2/(2R + T_{BS}/R_{BS})](P_1h\nu B) \end{aligned} \quad (21)$$

to be compared to the single-channel $\text{SNR}_{P_1}^2 = P_1/2h\nu B$, where the final result

$$F = (\text{SNR}_{P_2-P_1}/\text{SNR}_{P_1})^2 = 2/(R + T_{BS}/2R_{BS}). \quad (22)$$

From Eq. (22), we can see that the BS affects severely the improvement factor F . Indeed, if we chose a 50/50 BS, F would be less than two. For the improvement to be comparable to $F = 2/R$ of the direct configuration (Fig. 2), we shall limit $T_{BS}/2R_{BS}$ to a fraction of R ; for example, taking $T_{BS} = 0.05$ to have $F = 7.8$ dB, or $T_{BS} = 0.10$ for $F = 7.5$ dB. At these low values of transmittance, almost all of the power of the M1 output is taken by the PD, and only a small fraction of T_{BS} is used to sense the remote target. As a consequence, the SMI signal is decreased, and the performance is worsened, so that the improvement of F of the differential output becomes illusory.

The second method, consisting of sampling the outgoing beam by removing a small portion of it by means of a totally reflecting prism (or a mirror) is depicted in Fig. 5.

The power collected by this arrangement is the ratio of areas a' and $a + a'$ of the intercepted beam and the total beam, or $P_{1P} = [a'/(a + a')]P_1$ (Fig. 5). However, at equal $a'/(a + a')$ and R_{BS} , the fractional pickup of the beam is dramatically different from the BS pickup, because it does not open the port to the vacuum fluctuations (as the BS in Fig. 4 does). This is due to the total reflection of the prism (or of a mirror in place of it) that makes the arrangement a two-port device instead of the four ports of the BS (Fig. 4).

Therefore, for this configuration, the expressions of variance [Eqs. (12) and (13)] hold with P_1 replaced by P_{1P} , and the variance ratio of the signal difference [Eq. (14)] and the improvement [Eqs. (15) and (16)] also apply.

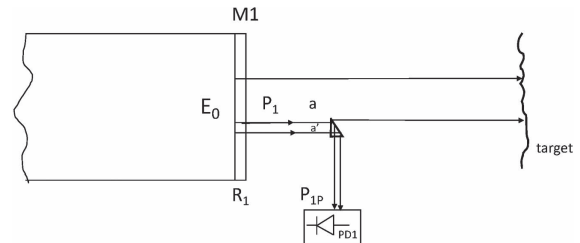


Fig. 5. Portion a' of the beam outgoing from mirror M1 by means of a reflecting prism.

4. Experimental Validation

We carried out the experiment with a 650 nm diode laser, Roithner QL65D6SA with a Fabry–Perot structure. The laser had a threshold of 30 mA and was biased at 40 mA and emitted at 5 mW. The monitor PD incorporated in the package supplied a 0.2 mA current, so it was receiving only about 10% of the power emitted by the rear mirror. This simplified the balancing operation with the $10\% = a'/(a + a')$ power picked up by a 3.1 mm side rectangular prism on the beam of about $w_0 = 10$ mm at the exit of an $F = 5$ mm, $NA = 0.53$ collimating lens. PD1 was fed to a transimpedance amplifier with $R_{f1} = 4.7$ k Ω feedback resistance and PD2 to another transimpedance amplifier feedback resistance R_{f2} adjustable between 1 and 10 k Ω . A difference operational amplifier provided a signal proportional to $P_{P1} - P_2$, and its output was directly sent to a digital oscilloscope. The target was a loudspeaker placed at 10 cm distance, with the central part covered by plain white paper. To balance the two channels, we applied a 1.5 mA triangular waveform to the bias current and adjusted R_{f2} so as to reach the condition of equal amplitude, or near to zero difference, as shown in Fig. 6.

Then, we analyze the difference signal $P_{P1} - P_2$ and its fluctuations, both in the frequency domain by means of a spectrum analyzer and as a total amplitude by means of an ac-coupled rms voltmeter.

In Fig. 7, we report the result of spectral noise measurement of the two channels P_{P1} and P_2 , and of their differential fluctuation, which is 2.5 dB smaller. Taking account of the doubling of signals [which amounts to 6 dB for their square, see Eq. (22)], the SNR improvement is $2.5 + 6 = 8.5 \pm 1$ dB.

We have also measured the total amplitude fluctuations of the two channels and of their difference and found that the improvement is even better than that recorded by the spectral density, typically of 2–3 dB. This is due to the presence, on both channels, of electrical disturbance (i.e., electromagnetic interference, EMI) and the $1/f$ noise component collected almost equally by both channels and obviously cancelled by the difference operation. For example, in Fig. 8, we report an example of the SMI channels deliberately disturbed by an EMI perturbation generated by the

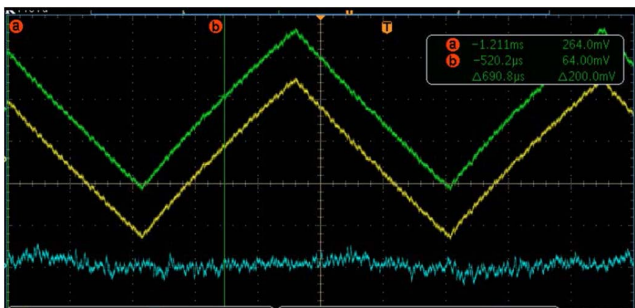


Fig. 6. Balancing of the two SMI signals detected by PD1 and PD2: a triangular waveform is applied to the bias and generates detected responses brought to be nearly identical [top trace], that is, with a residually small difference [bottom trace].

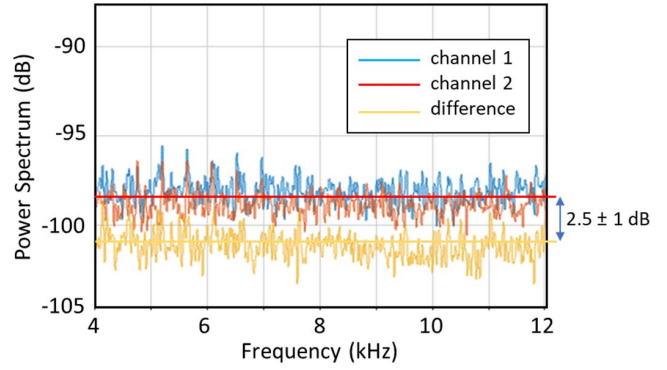


Fig. 7. Signals detected by PD1 and PD2 (red and blue) and their difference (yellow), exhibiting a noise 2.5 ± 1 dB smaller.

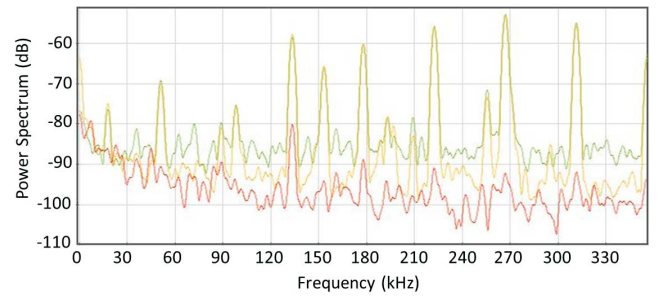


Fig. 8. Peaks of EMI superposed to the SMI of channels PD1 and PD2 (yellow and yellow-green) and the difference channel (red), exhibiting a disturbance reduction of 25 . . . 30 dB.

brushes of an electrical motor placed in close proximity to the optical SMI. The series of peaks at frequencies from 30 to 300 kHz are reduced in amplitude by about 25 to 30 dB thanks to the difference operation.

5. Conclusions

We have demonstrated that the difference signal of the two outputs—front and rear—of a laser diode SMI has an improved SNR with respect to each of the two outputs. On a Fabry–Perot laser, we have measured an improvement of 8.5 ± 1 dB, which is in good agreement with the theoretical value of 8.2 dB. We have also found that EMI collected by the two channels is strongly reduced (of 25–30 dB) by the difference operation. The improvement is due to the two signals being in phase opposition above the threshold and to the partial correlation of the noises as shown by an analysis based on a second-quantization model.

Appendix A

Let us make some exemplary cases calculating the values of $m_{1,2}$ normalized to $(t_1^2/r_1)(A \cos \phi)$ using Eqs. (3) and (4). Let us assume for our semiconductor laser diode that $R_{1,2} = 0.3$,

Table 1. Modulation Indices and Signal Amplitudes.

$2\gamma L$	2.40×1.1 (10% above threshold)	3.60 (50% above threshold)	4.80 ($\times 2$)	5.40 ($\times 2.25$)	6.00 ($\times 2.5$)	7.20 ($\times 3$)	9.60 ($\times 4$)
m_2 (rear)	4.17	0.83	0.42	0.33	0.28	0.21	0.114
m_1 (front)	3.74	0.40	-0.01	-0.10	-0.15	-0.22	-0.316
Signal difference	0.43	0.43	0.43	0.43	0.43	0.43	0.43
Ratio of difference to semi-sum	0.11	0.70	2.0	2.0	2.0	2.0	2.0

so that $\ln R_1 R_2 = -2.40$, and $R_1/T_1 = 0.428$. At threshold, $2\gamma L = -\ln R_1 R_2 = 2.40$. Then, we have, at various values of round-trip gain, $2\gamma L$, as shown in Table 1.

As we can see, when signal m_1 changes sign, the ratio of difference to the semi-sum of amplitudes (the absolute values of m) becomes equal to two.

References

1. S. Donati, "Developing self-mixing interferometry for instrumentation and measurements," *Laser Photon. Rev.* **6**, 393 (2012).
2. S. Donati, *Electro-Optical Instrumentation—Sensing and Measuring with Lasers* (Prentice Hall, 2004).
3. S. Donati and M. Norgia, "Overview of self-mixing interferometer applications to mechanical engineering," *Opt. Eng.* **57**, 051506 (2018).
4. P. Dean, Y. L. Lim, A. Valavanis, R. Kleise, M. Nikolic, D. Indjin, Z. Ikonik, P. Harrison, A. D. Rakic, E. H. Lindfield, and G. Davies, "Terahertz imaging through self-mixing in a quantum cascade laser," *Opt. Lett.* **36**, 2587 (2011).
5. E. Randone and S. Donati, "Self-mixing interferometer: analysis of the output signals," *Opt. Express* **14**, 9788 (2006).
6. K. Li, F. Cavedo, A. Pesatori, C. Zhao, and M. Norgia, "Balanced detection for self-mixing interferometry," *Opt. Lett.* **42**, 283 (2017).
7. S. Donati, *Photodetectors—Devices, Circuits and Applications*, 2nd ed. (Wiley and IEEE, 2021), p. 427.
8. J. L. Vey, K. Auen, and W. Elsasser, "Intensity fluctuation correlations for a Fabry–Perot semiconductor laser: a semiclassical analysis," *Opt. Commun.* **146**, 325 (1998).
9. R. J. Fronen, "Correlation between $1/f$ fluctuations in the two output beams of a laser diode," *J. Quantum. Electron.* **27**, 931 (1991).